

## Supplementary Information

### **Orthogonal Small-Molecule Zinc Porphyrin Derivative as Efficient Hole Transport Material for High-performance Inverted Perovskite Solar Cells**

Chaojun Sun, Lunan Du, Wenxiu Du, Jingsheng Wang, Huiru Li, Youtian Tao\*,  
Zhengyi Sun\*

Key Laboratory of Flexible Electronics & Institute of Advanced Materials, School of Flexible Electronics (Future Technologies), Nanjing Tech University, 30 South Puzhu Road, Nanjing 211816, China

\*Corresponding author: [iamy tao@njtech.edu.cn](mailto:iamy tao@njtech.edu.cn); [iamzysun@njtech.edu.cn](mailto:iamzysun@njtech.edu.cn)

## Experimental section

### 1. Materials

All reagents and chemicals were purchased from commercial sources and used without further purification unless stated otherwise.

### 2. Synthesis of ZnP-4ThDPP

The synthetic routes for ZnP-4ThDPP are presented in Figure 1, with the detailed synthetic procedures based on our previous work published in *Dyes and Pigments* 2021, 188, 109216.

### 3. Preparation of perovskite solar cells

#### I. Cleaning of ITO conductive glass

ITO conductive glass with a dimension of 12×12 mm<sup>2</sup> and thickness of 1.1 mm was selected as the substrate, on which the ITO film with a thickness of 150 nm is etched into a U-shaped pattern with a width of 2 mm. By combining with the top-electrode with a width of 2 mm, the effective area of PSC device was thereby controlled to be 4 mm<sup>2</sup>. The cleaning steps were as follows. First, the substrate was scrubbed with cleaning agent and deionized water. Then, acetone and isopropanol ultrasound separately for 15 minutes on the Teflon cleaning rack. After that, check the glass surface by achieving uniform and continuous water film. Finally, after drying by vacuum drying oven, ultraviolet ozone treatment for 20 min to enhance the surface wettability of substrate and increase the work function of ITO.

#### II. Preparation of hole transport layer

##### ZnP-4ThDPP film

1.5 mg ZnP-4ThDPP was weighed and dissolved in 800 μL CB and 200 μL CF<sub>3</sub>, and stirred at 60 °C for 2 h. The solution was spin-coated on the ITO glass substrate at 4000 rpm for 30 s and then annealed at 60 °C for 10 min.

##### Li-TFSI doped ZnP-4ThDPP film

The ZnP-4ThDPP solution was prepared as mentioned above and set aside for standby. Separately, 260 mg of LiTFSI was weighed to prepare a 520 mg/mL acetonitrile solution, which was added to the ZnP-4ThDPP solution in varying volumes. The spin-coating parameters were set to 5000 rpm for 30 seconds. During the spin-

coating process, once the substrate reached a rotation speed of 5000 rpm, a drop of ZnP-4ThDPP solution was quickly added to rapidly form a film. After spin-coating, the sample was immediately placed on a hot plate at 60 °C for annealing for 10 min. A gradient experiment was conducted with the volume of the Li-TFSI solution added as the variable. The final doping ratio was determined to be 14  $\mu\text{L}$  of the LiTFSI acetonitrile solution added in 1000  $\mu\text{L}$  of ZnP-4ThDPP solution.

#### **NiO<sub>x</sub> film**

1000  $\mu\text{L}$  ethylene glycol and 67  $\mu\text{L}$  hexanediamine were added to 290.7 mg Ni(NO<sub>3</sub>).6H<sub>2</sub>O and stirred at 60 °C for 2 h. The solution was spin-coated on the ITO glass substrate by the two-step spin coating method (600 rpm @8 s + 2500 rpm @80 s) and then gradient annealed at 300 °C for 60 min.

#### **III. Preparation of perovskite layer**

171.97 mg FAI, 22.39 mg MABr, 80.74 mg PbBr<sub>2</sub>, 507.11 mg PbI<sub>2</sub> were dissolved in 800  $\mu\text{L}$  DMF and 200  $\mu\text{L}$  DMSO, and then added 45  $\mu\text{L}$  CsI solution (194.86 mg CsI dissolved in 500  $\mu\text{L}$  DMSO). Finally, stirring at 60 °C for 2 h. The solution was spin-coated on the substrate by the two-step spin coating method (1000 rpm @10 s + 5000 rpm @27 s) and then annealed at 90 °C for 10 min.

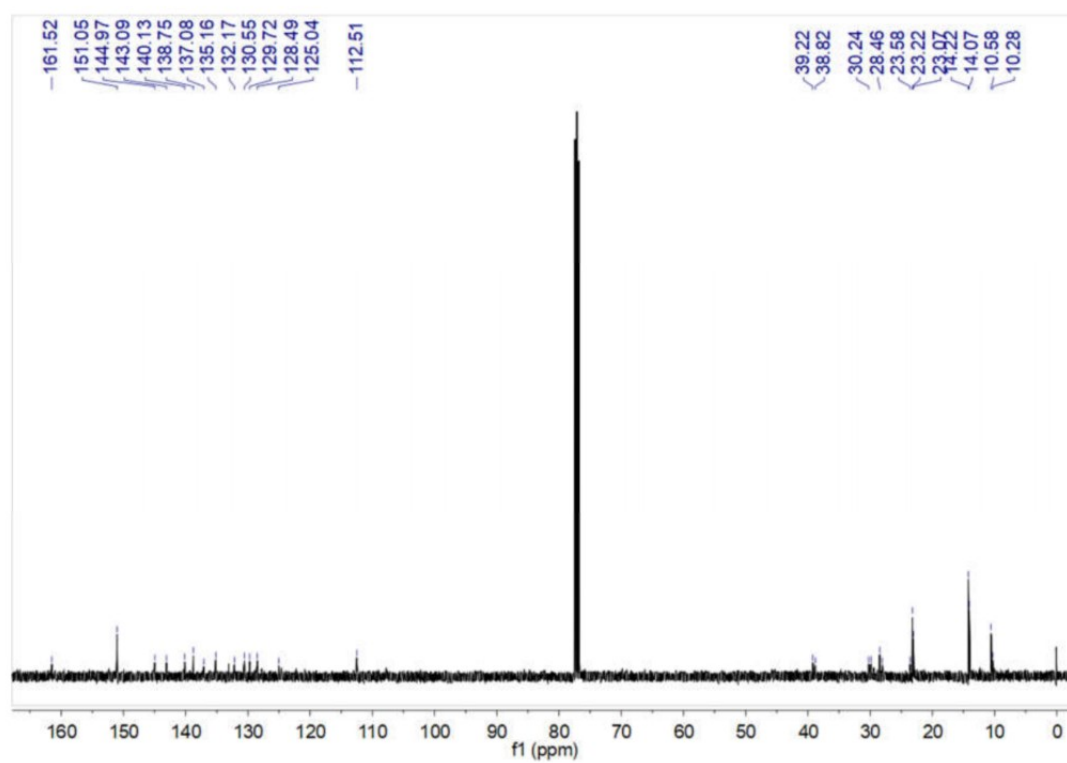
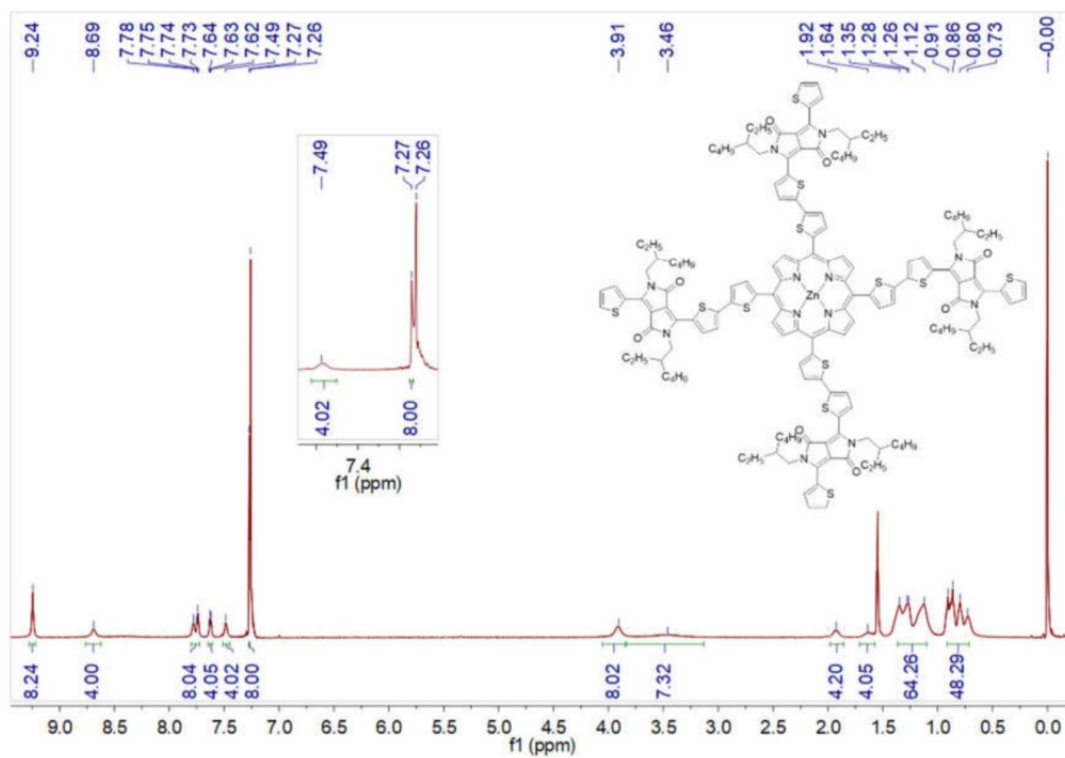
#### **IV. Preparation of electron transport layer and top electrode**

We prepared 20 nm C<sub>60</sub>, 6 nm BCP and 100 nm Ag separately by thermal evaporation in a vacuum chamber under  $5 \times 10^{-5}$  Pa.

#### **5. Characterization of perovskite solar cells**

The surface morphology of the films was characterized by using the SEM (JEOL, JSM-7800F) and the AFM (Park, XE-70). The crystal structure of the films was analyzed by using an X-ray diffractometer with Cu K $\alpha$  radiation (Smartlab). PL spectra and TRPL spectra were measured by a PL spectrometer (Edinburgh Instruments, FLS980) with an excitation wavelength of 520 nm. The device performance of PSCs was characterized in a nitrogen glovebox with a source-measure unit (Tektronix, Keithley 2400) under a solar simulator (Enlitech, SS-F5-3A) with AM 1.5G and 100 mW cm<sup>-2</sup>. The devices were tested in forward and reverse scan mode, from -0.2 V to 1.2 V and from 1.2 to -0.2 V, respectively, with a 0.02 V step. The contact angle measurement was carried out by KRUSS GmbH DSA1005 system.

## Supplementary Figures



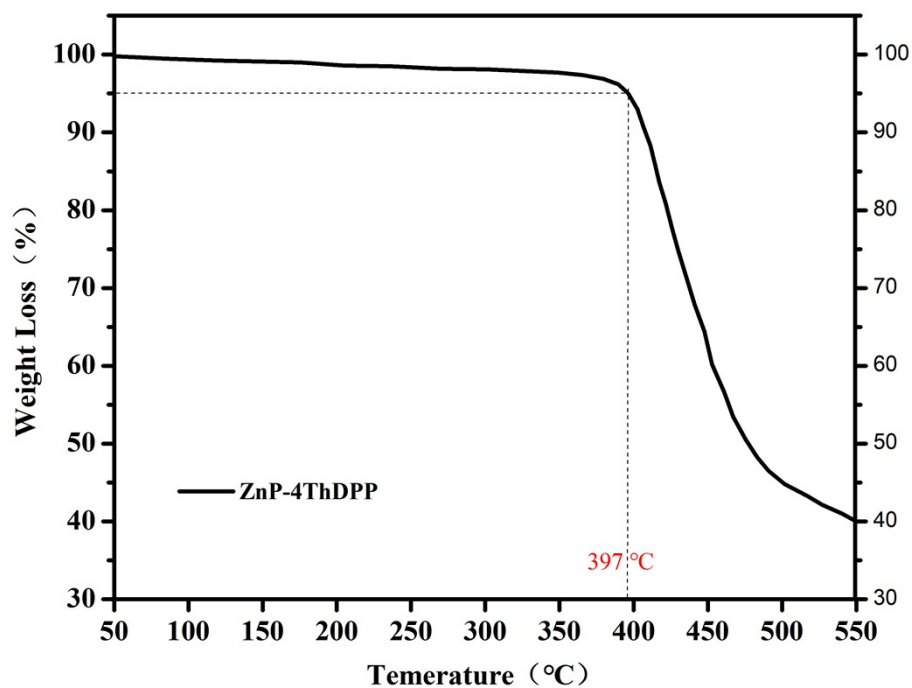


Figure S3. TGA curve of ZnP-4ThDPP.<sup>[1]</sup>

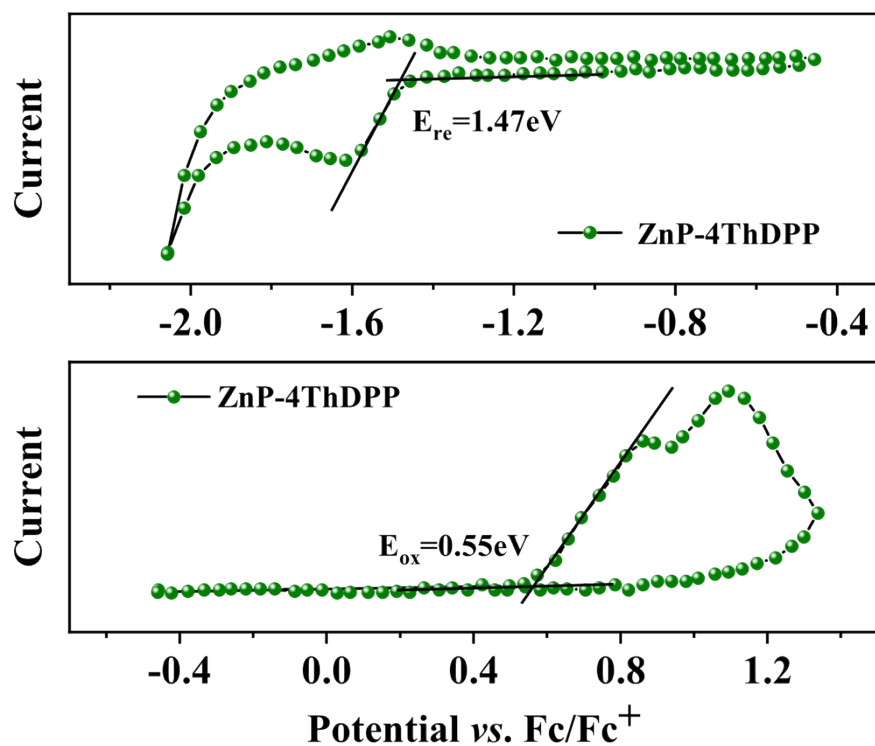
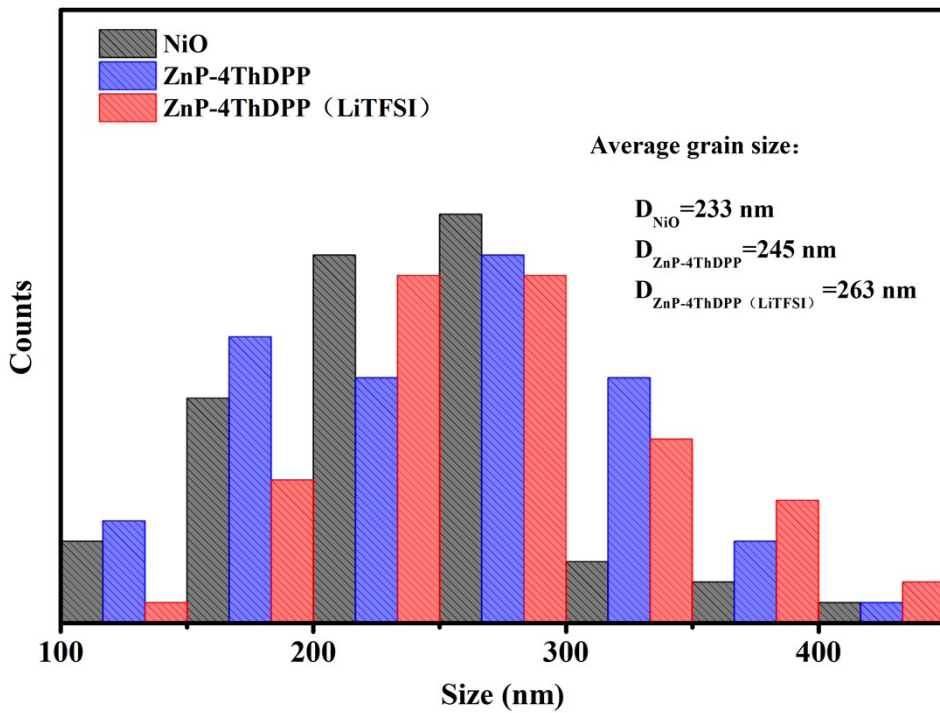
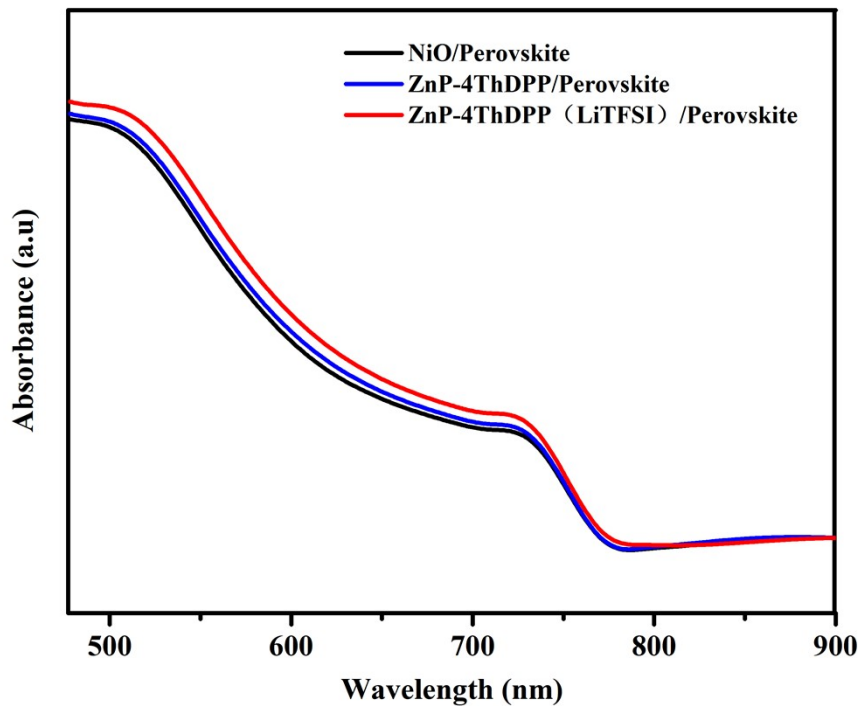


Figure S4. CV curves of oxidation and reduction process for ZnP-4ThDPP.<sup>[1]</sup>



**Figure S5.** The grain size distribution of perovskite films deposited on NiO<sub>x</sub>, ZnP-4ThDPP and ZnP-4ThDPP doped with LiTFSI. Data was obtained using a specific software named Nano Measurer.



**Figure S6.** Absorbance of perovskite films prepared on NiO<sub>x</sub>, ZnP-4ThDPP and LiTFSI-doped ZnP-4ThDPP HTLs.

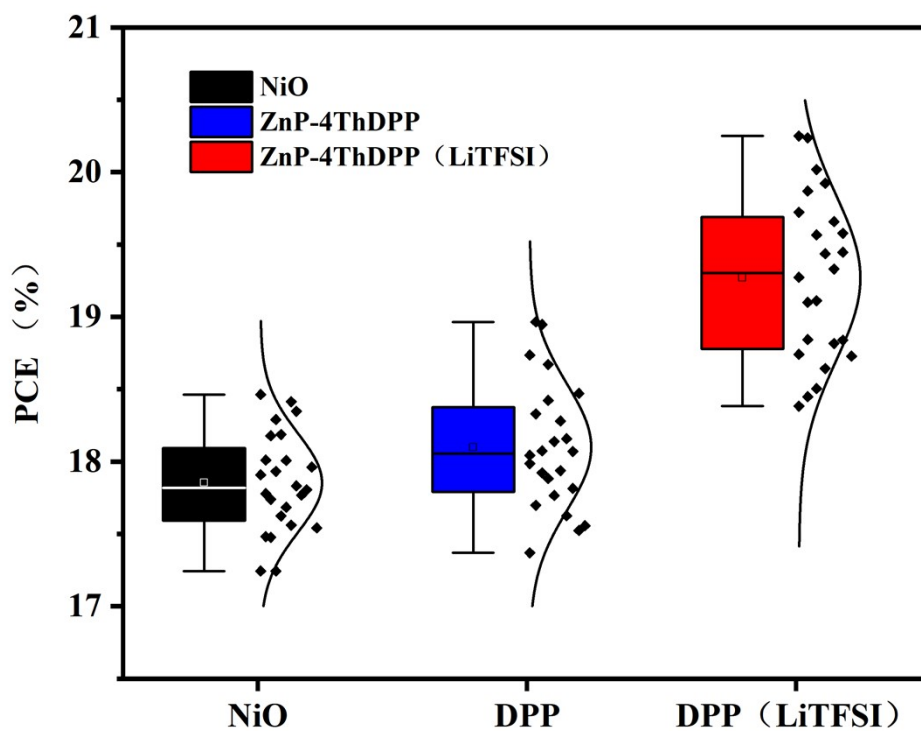


**Figure S7.** PCE distribution diagram of PSCs based on NiO<sub>x</sub>, ZnP-4ThDPP and LiTFSI-doped ZnP-4ThDPP HTLs, with box plots and the standard deviation shown alongside the data points, collected from 24 devices, respectively.

**Table S1.** A summary of zinc porphyrin derivatives as HTMs in PSCs.

Ref.	Zinc porphyrin derivatives	Device architecture with zinc porphyrin HTM	Device type	Role	PCE (%)	Year
[2]	Y2, Y2A2	ITO/TiO <sub>2</sub> /MAPbI <sub>3</sub> /HTM/Au	conventional	HTL	16.6, 10.55	2016
[3]	PZn-TPA, PZn-DPPA series	ITO/ZnO/MAPbI <sub>3</sub> /HTM/Au	conventional	HTL	11.96-14.11	2017
[4]	ZnP	FTO/c-TiO <sub>2</sub> /m-TiO <sub>2</sub> /(FAPbI <sub>3</sub> ) <sub>0.85</sub> (MAPbBr <sub>3</sub> ) <sub>0.15</sub> /ZnP/Au	conventional	HTL	17.78	2017
[5]	DPPZnP-TSEH	FTO/SnO <sub>2</sub> :C60/MAPbI <sub>3</sub> /DPPZnP-TSEH/MoO <sub>3</sub> /Ag	conventional	HTL	9.38	2017
[6]	ZnBChI, ZnChI, ZnPor	FTO/c-TiO <sub>2</sub> /m-TiO <sub>2</sub> /MAPbI <sub>3</sub> /HTM/Ag	conventional	HTL	8.26, 11.88, 0.68	2018
[7]	WT3, YR3	FTO/c-TiO <sub>2</sub> /m-TiO <sub>2</sub> /Cs <sub>0.05</sub> (FA <sub>0.83</sub> MA <sub>0.17</sub> ) <sub>0.95</sub> PbI <sub>0.83</sub> Br <sub>0.17</sub> /HTM/Au	conventional	HTL	19.44, 17.84	2018
[8]	PZn-2FTPA	ITO/ZnO-S/MAPbI <sub>3</sub> /PZn-2FTPA/Au	conventional	HTL	18.85	2018
[9]	ZnPy	FTO/TiO <sub>2</sub> /MAPbI <sub>3</sub> /ZnPy/Au	conventional	HTL	17.82	2019
[10]	ZPPHT	FTO/c-TiO <sub>2</sub> /m-TiO <sub>2</sub> /MAPbI <sub>3</sub> /ZPPHT/Carbon	conventional	HTL	11.26	2019
[11]	Y4	FTO/c-TiO <sub>2</sub> /m-TiO <sub>2</sub> /(FA) <sub>0.85</sub> (MA) <sub>0.15</sub> Pb(I <sub>3</sub> ) <sub>0.85</sub> (Br <sub>3</sub> ) <sub>0.15</sub> /Y4/Au	conventional	HTL	16.05	2019
[12]	ZnPc3	FTO/c-TiO <sub>2</sub> /m-TiO <sub>2</sub> /(MAPbBr <sub>3</sub> ) <sub>0.15</sub> (FAPbI <sub>3</sub> ) <sub>0.85</sub> /ZnPc3/Au	conventional	HTL	18.32	2022
[13]	ZnPor	FTO/c-TiO <sub>2</sub> /m-TiO <sub>2</sub> /MAPbI <sub>3</sub> /(ZnPor/rGO/CuO nanocomposite)/Carbon <sup>bio</sup>	conventional	HTL	9.8	2022
[14]	MDA4, MTA4, MDA8	(FTO/SnO <sub>2</sub> /FA <sub>0.8</sub> MA <sub>0.2</sub> PbI <sub>3</sub> /p-FPEAI/HTM/Au	conventional	HTL	22.67, 12.32, 14.64	2022
[15]	Zn-PP	FTO/SnO <sub>2</sub> /FA <sub>0.95</sub> MA <sub>0.05</sub> PbI <sub>2.85</sub> Br <sub>0.15</sub> /Zn-PP/Spiro-OMeTAD/Au	conventional	buffer in antisolvent	19.11	2024
[16]	(ZnP) <sub>n</sub> (polymerized)	FTO/ZnO-MgO-EA <sup>+</sup> /m-TiO <sub>2</sub> /Cs <sub>x</sub> (MA <sub>0.17</sub> FA <sub>0.83</sub> ) <sub>(1-x)</sub> Pb(I <sub>0.83</sub> Br <sub>0.17</sub> ) <sub>3</sub> /(ZnP) <sub>n</sub> / Spiro-MeOTAD/Au	conventional	buffer in antisolvent	20.53	2022

[17]	Zn-porphyrin	ITO/PEDOT:PSS/Zn-porphyrin/MAPbI <sub>3</sub> /PCBM/C60/BCP/Al	inverted	buffer layer	14.05	2016
[18]	m-PYBrZnPor	ITO/PTAA/MAPbI <sub>3</sub> /PCBM/m-PYBrZnPor/Ag	inverted	buffer layer	17.5	2018
[19]	PZnP (polymerized)	ITO/PZnP/MAPb(I <sub>0.95</sub> Cl <sub>0.05</sub> ) <sub>3</sub> /PCBM/PEI/Ag	inverted	HTL	19.75	2023

## References

- [1] X. Gao, Y. Wu, X. Song, X. Tao, Y. He, T. Yang, R. Yu, Z. Li, Y. Tao, *Dyes and Pigments* 2021, 188, 109216.
- [2] H. H. Chou, Y. H. Chiang, M. H. Li, P. S. Shen, H. J. Wei, C. L. Mai, P. Chen and C. Y. Yeh, *ACS Energy Letters*, 2016, 1, 956-962.
- [3] U. H. Lee, R. Azmi, S. Sinaga, S. Hwang, S. H. Eom, T. W. Kim, S. C. Yoon, S. Y. Jang and I. H. Jung, *ChemSusChem*, 2017, 10, 3780-3787.
- [4] S. Chen, P. Liu, Y. Hua, Y. Y. Li, L. Kloo, X. Z. Wang, B. Ong, W. K. Wong and X. J. Zhu, *ACS Applied Materials & Interfaces*, 2017, 9, 13231-13239.
- [5] K. Gao, Z. L. Zhu, B. Xu, S. B. Jo, Y. Y. Kan, X. B. Peng and A. K. Y. Jen, *Advanced Materials*, 2017, 29, 201703980
- [6] M. Z. Li, N. Li, W. D. Hu, G. Chen, S. Sasaki, K. Sakai, T. Ikeuchi, T. Miyasaka, H. Tamiaki and X. F. Wang, *ACS Applied Energy Materials*, 2018, 1, 9-16.
- [7] Y. H. Chiang, H. H. Chou, W. T. Cheng, Y. R. Li, C. Y. Yeh and P. Chen, *ACS Energy Letters*, 2018, 3, 1620-1626.
- [8] R. Azmi, U. H. Lee, F. T. A. Wibowo, S. H. Eom, S. C. Yoon, S. Y. Jang and I. H. Jung, *ACS Applied Materials & Interfaces*, 2018, 10, 35404-35410.
- [9] X. D. Lv, G. B. Xiao, X. X. Feng, J. Cao, X. Q. Yao and J. C. Liu, *Dyes and Pigments*, 2019, 160, 957-961.
- [10] G. Reddy, R. Katakam, K. Devulapally, L. A. Jones, E. Della Gaspera, H. M. Upadhyaya, N. Islavath and L. Giribabu, *Journal of Materials Chemistry C*, 2019, 7, 4702-4708.
- [11] W. Zhang, Y. Hua, L. Q. Wang, B. B. Zhang, Y. Y. Li, P. Liu, V. Leandri, Y. Guo, H. Chen, J. M. Gardner, L. C. Sun and L. Kloo, *ACS Applied Energy Materials*, 2019, 2, 6768-6779.

- [12] M. Pegu, D. Molina, M. J. Alvaro-Martins, M. Castillo, L. Ferrer, P. Huang, S. Kazim, A. Sastre-Santos and S. Ahmad, *Journal of Materials Chemistry C*, 2022, 10, 11975-11982.
- [13] F. Arjmand, S. J. Fatemi, S. Maghsoudi and A. Naeimi, *Journal of Materials Research and Technology*, 2022, 16, 1008-1020.
- [14] C. Mai, Q. Xiong, X. Li, J. Chen, J. Chen, C. Chen, J. Xu, C. Liu, C. Yeh, and P. Gao, *Angew. Chem. Int. Ed.* 2022, 61, e202209365
- [15] A. K. K. Soopy, B. Parida, S. A. Aravindh, H. SahulHameed, B. S. Swain, N. i. Saleh, I. M. A. Taha, D. H. Anjum, V. Alberts, S. Liu and A. Najjar, *Solar RRL* 2024, 8, 2400054.
- [16] H. X. Liang, W. D. Wang, S. B. Mai, X. D. Lv, J. Fang and J. Cao, *Chemical Engineering Journal*, 2022, 429, 132405.
- [17] B. B. Li, C. Y. Zheng, H. Liu, J. Zhu, H. M. Zhang, D. Q. Gao and W. Huang, *ACS Applied Materials & Interfaces*, 2016, 8, 27438-27443.
- [18] Y. Liu, J. Qi, X. B. Peng and Y. Cao, *Organic Electronics*, 2018, 59, 414-418.
- [19] Y. J. Lan, Y. D. Wang, Z. R. Lan, Y. Wang, B. B. Cui, J. Y. Shao and Y. W. Zhong, *Journal of Materials Chemistry A*, 2023, 11, 7085-7093.